Int. J. Electrochem. Sci., 6 **(2011)** 5741 - 5758

International Journal of
ELECTROCHEMICAL
SCIENCE
www.electrochemsci.org

Electrodeposited Cu–CuO Composite Films for Electrochemical Detection of Glucose

H. B. Hassan[1,*], *Z. Abdel Hamid*[2]

[1] Faculty of Science, Department of Chemistry, Cairo University, Giza, Egypt
[2] Central Metallurgical Research & Development Institute (CMRDI), Helwan, Egypt
[*]E-mail: Hanaa20055@hotmail.com

Received: 21 September 2011 / *Accepted:* 18 October 2011 / *Published:* 1 November 2011

Cu–CuO composite films were deposited onto carbon electrodes by electrodeposition technique via a noncyanide alkaline electrolyte containing mannitol [$C_6H_8(OH)_6$] as a complexing agent. Scanning electron microscopy (SEM), energy dispersive X-ray system (EDX) and X-ray diffraction (XRD) were used to assess the surface characterizations of the fabricated composite films. The results reveal that the distribution of the CuO particulates in the matrix allowed the formation of fine-grained composite film. The catalytic activity of the Cu–CuO/C prepared electrodes towards electrooxidation of glucose in alkaline medium compared to those of the massive Cu and electrodeposited Cu/C electrodes has been evaluated using electrochemical measurements. The electrodeposited Cu–CuO/C composite films show higher catalytic activity and stability towards electrooxidation of glucose compared to the massive Cu and electrodeposited Cu/C electrodes. The performance of the Cu–CuO/C anodes towards electrooxidation of glucose increases with increasing the wt.% of CuO in the deposited film up to 25 wt.%. The sensitivity of Cu–CuO /C (25 wt.% CuO) electrode was estimated showing a linear range up to 3 mM with sensitivity of 598 μA cm^{-2} mM^{-1} and detection limit of 5 μM. At the optimum oxidation potential, the fabricated electrode was highly selective to glucose in the presence of ascorbic acid as a common interfering species in biological fluids.

Keywords: Copper electrodeposition; Environmental electrolytes; Cu composite; Free cyanide electrolyte; Glucose electrooxidation

1. INTRODUCTION

For many years, Cu and Cu–based electrodes have been used extensively as anodes in electrooxidation of some organic compounds [1–6]. Some types of these electrodes showed an excellent electrocatalytic activity for glucose oxidation without observable self-poisoning [7, 8]. Over the past few decades, a great attention has been paid to the development of electrochemical glucose sensors. This is ascribed to the essentiality of reliable and fast monitoring of glucose in the fields of

biotechnology, clinical diagnostics and food industry. A large number of transition metal and transition metal oxide electrodes as well as some alloys or composite electrodes have shown a good degree of electroactivity toward glucose oxidation [9–11]. However, a majority of glucose sensors depends on Cu and Cu oxide nanomaterials for the non-enzymatic detection of glucose. Especially CuO or Cu_2O modified electrodes that exhibited outstanding catalytic activity towards glucose electrooxidation [12, 13]. The electrooxidation process follows the formation of Cu(III) and is catalyzed by this species through a mediated electron transfer mechanism [1]. It was found that the biosensor based on Cu_xO/Cu prepared by different techniques exhibited excellent performance for glucose detection, giving a linear dependence between current and glucose concentrations with a low detection limit and high sensitivity [14, 15].

Also, CuO flowers and nanorods synthesized on graphite substrates exhibited excellent catalysis to direct glucose oxidation [16]. Additionally, Cu oxide film prepared by electroless Cu plating followed by chemical oxidation on spherical glass beads [17] and Cu oxide/hydroxide nanoparticles highly dispersed in graphite-like carbon film (Cu–NDC) by RF co-sputtering Cu displayed good catalytic activity and stability towards glucose oxidation in alkaline medium [18]. On the other hand, Cu–nanocomposites such as Cu–C and Cu–ZnO have been explored extensively due to their unique physical and chemical properties. They showed good non–enzymatic electrocatalytic responses for glucose in alkaline media with a high sensitivity, stability and reproducibility [3, 19]. The electrocatalytic activity of the Cu composite electrode towards glucose may be attributed to the involvement of Cu(II) and Cu(III) surface species in the oxidation of glucose in alkaline medium [20].

Several studies have been reported on the fabrication techniques of copper–based electrodes for glucose sensing. However, the method of fabrication may be cumbersome; therefore, a reliable, sensitive and selective electrode which can be fabricated by a simple procedure remains a challenge for researchers.

Therefore, herein a simple electrodeposition technique will be used for preparation of Cu based composite electrodes. It is well established that Cu or Cu based films can be deposited from two main types of electrolyte solutions, the alkaline cyanide Cu and the acid sulfate Cu [21, 22]. But the use of cyanide salts in Cu plating electrolytes has become environmentally disfavored because of ecological considerations.

Accordingly, noncyanide electrolytes for Cu plating have been proposed for use as replacements for the well-known cyanide counterparts [23]. Therefore, this work aims to use an environmentally friendly alkaline electrolyte containing mannitol as a complexing agent to prepare Cu–CuO composite materials in an attempt to enhance the electrocatalytic activity of Cu towards glucose electrooxidation. In order to prepare highly dispersed Cu based electrodes with improved catalytic activity, electrodeposited Cu–CuO composite films supported on carbon electrodes have been prepared by a facile electrodeposition technique. Various amount of CuO was introduced into the plating electrolyte to study the effect of changing CuO content on the performance of the fabricated composite electrodes towards glucose electrooxidation. A massive Cu and the electrodeposited Cu/C were used for a comparative study.

2. EXPERIMENTAL TECHNIQUES

2.1. Electrochemical measurements

Electrochemical measurements were performed on a massive Cu electrode and modified carbon electrodes; each has a surface area of 0.125 cm^2. The carbon electrodes were modified by electrodeposited Cu or Cu–CuO composite films. Before the electrodeposition process, the massive Cu and carbon electrodes were mechanically polished using emery papers of various grades, then they were subsequently degreased with acetone, rinsed with triply distilled water and dried with a soft tissue paper. The apparent surface area was calculated from the geometric area and the current density was referred to herein. The electrochemical cell used was a conventional three-electrode glass cell. The reference electrode is the [Hg / HgO / 1.0 M NaOH (MMO), E^o = 140 mV vs. NHE] and a Pt sheet was used as a counter electrode. Measurements were carried out in an aerated 0.25 M NaOH solution at room temperature of 25 ± 2 ^oC. The electrochemical measurements were performed using Amel 5000 system (supplied by Amel Instrument, Italy) driven by an IBM PC for data processing. The PC was interfaced with the instrument through a serial RS-232 card.

2.2. Electrodeposition technique

The electrodeposition of Cu or Cu–CuO on carbon electrodes was performed from a noncyanide electrolyte containing anhydrous copper sulphate ($CuSO_4$) 15 g L^{-1}, sodium hydroxide (NaOH) 120 g L^{-1} and mannitol ($C_6H_8(OH)_6$) 35 g L^{-1} as a complexing agent and (0– 10 g L^{-1}) CuO powder of an average particle size ~ 8 µm. The electrolyte was maintained at pH 12.5, operated at room temperature (25 °C) and current density 4 A dm^{-2}. Prior to the co-deposition, the CuO powder were stirred using magnetic stirrer at 150 rpm to get uniform suspension of particles in the solution and break up the agglomeration. Chemicals were obtained from Sigma-Aldrich, mannitol, D(+)–glucose and L–ascorbic acid and all other reagents were of analytical grade and were used as received without further purification. Triply distilled water was used throughout for the preparation of solutions.

2.3. Zeta potential measurements

Zeta potential measurements were carried out using Lazer Zetameter “Malven Instrument” model “Zetasizer2000”. 0.01 g CuO powder was immersed into volume of 50 ml of electroplating solution. The pH was adjusted at the desired value using NaOH or HCl solution. The sample was shaken for 30 min. and the zeta potential was measured.

2.4. Size Analysis of Samples

A Laser particle size analyzer "FRITSCH" model "Analystte 22", was employed for size analysis of CuO powder.

2.5. Surface analysis

The phase structure of the coatings was studied using X-ray diffractometry (BRUKER axc-D8) using CuKα radiation with λ = 0.1542 nm and operated at 45 KV and 40 mA. Scanning electron microscope (SEM-JEOL-5410) equipped with an energy dispersive X-ray analyser (EDX) was used to study the surface morphology and composition of the electrodeposited layers.

3. RESULTS AND DISCUSSION

3.1. Electrodeposition and characterization

Figure 1 illustrates typical top-view SEM images of the electrodeposited Cu and Cu–CuO composite films on carbon electrodes from a noncyanide alkaline electrolyte containing mannitol as a complexing agent operated at 4 A dm^{-2}, pH 12.5, 150 rpm, and 25 ^{o}C.

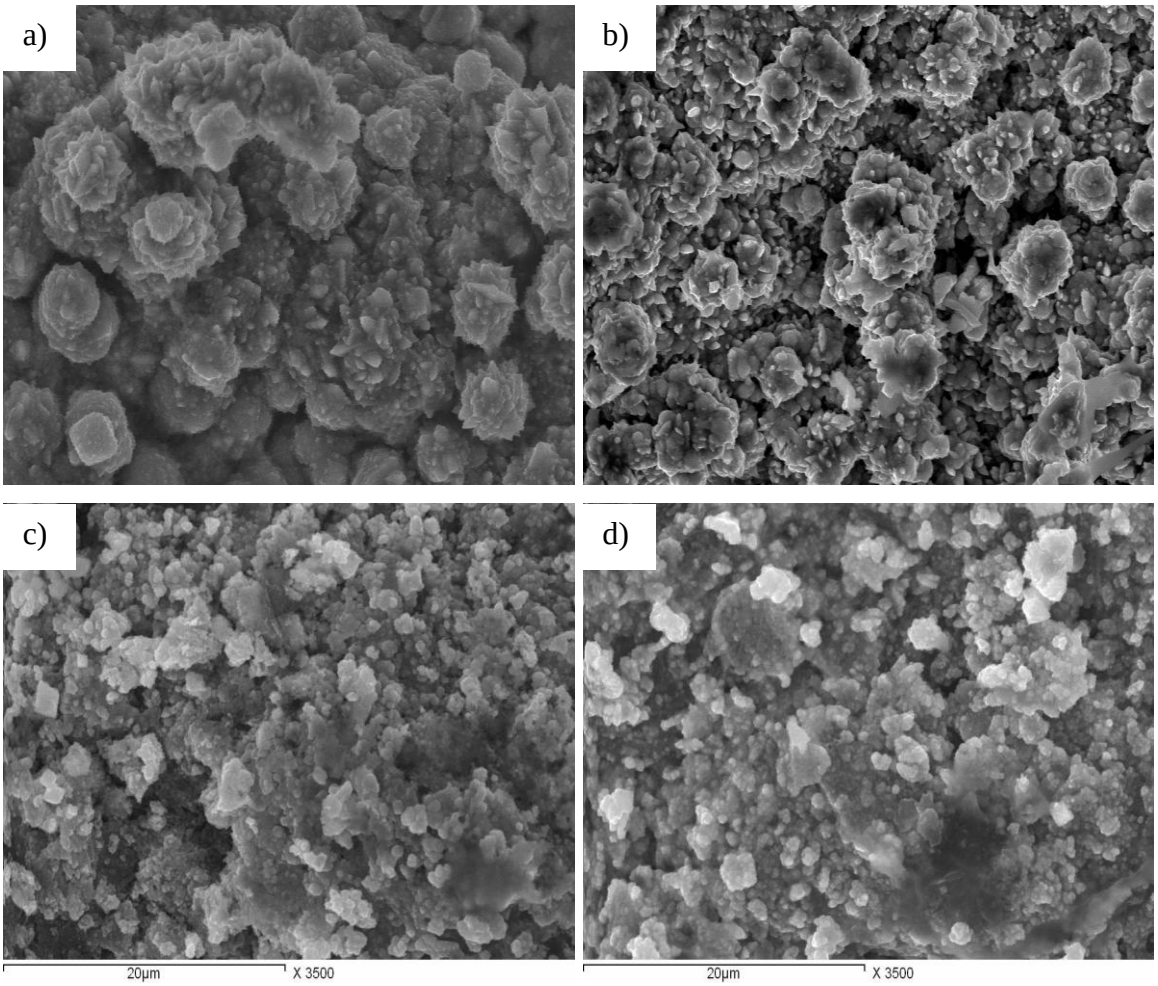

Figure 1. SEM images of Cu and Cu–CuO films deposited from a noncyanide alkaline electrolyte at 25 °C, 4 A dm^{-2}, 35 g L^{-1} mannitol concentration and containing different CuO contents: a) 0, b) 3, c) 5 and d) 10 g L^{-1}.

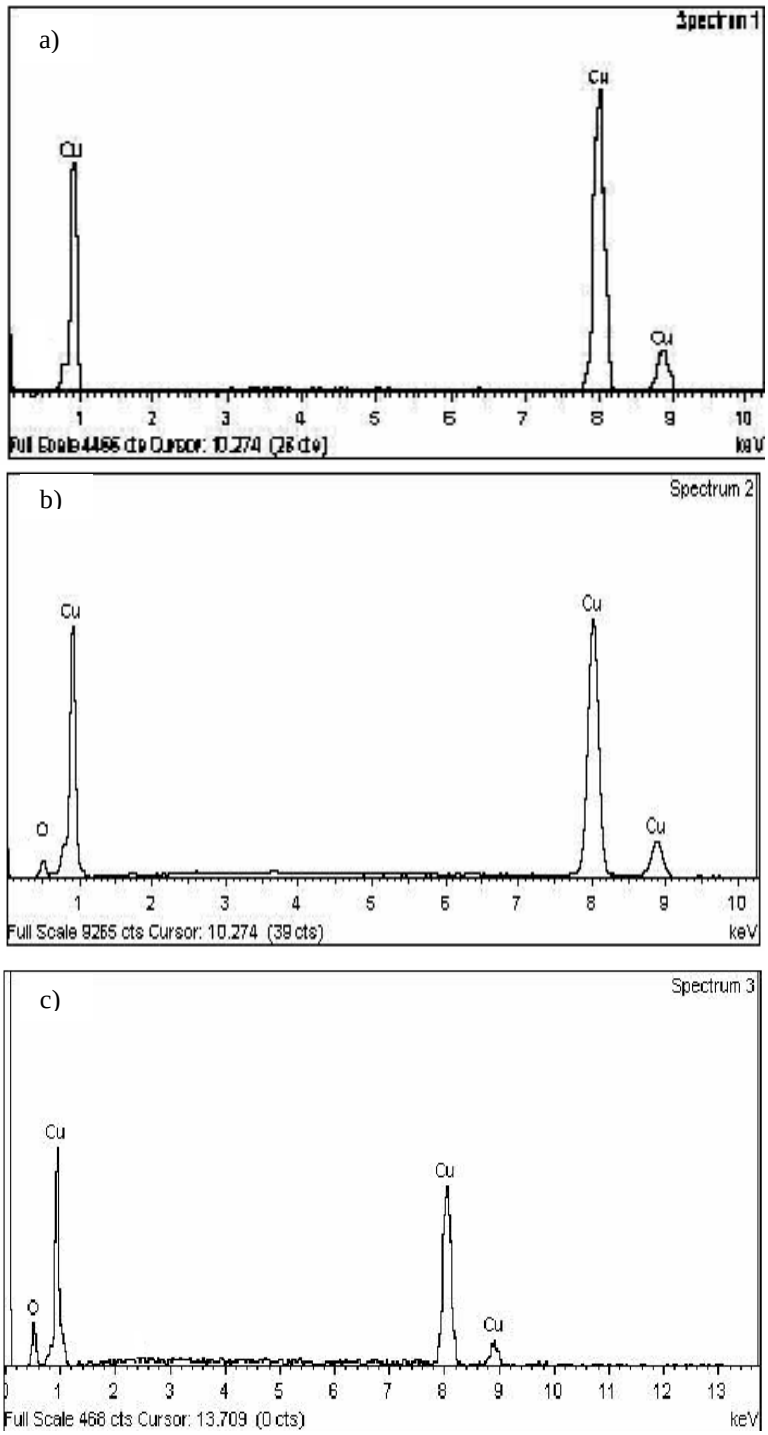

Figure 2. EDX spectrum of electrodeposited Cu and Cu–CuO films deposited from a noncyanide alkaline electrolyte at 25 °C, 4 A dm^{-2}, 35 g L^{-1} mannitol concentration and containing different CuO contents: a) 0, b) 3 and c) 5 g L^{-1}.

The thickness of each deposited layer is adjusted to be about 10 μm. The images reflect that the surface morphology of the electrodeposited Cu and Cu–CuO films has flowers-like structure in the form of clusters distributed over the entire surface. The influence of changing CuO contents in the

electrolyte on the surface morphology of Cu matrix is shown in Fig. 1b-d and EDX analysis has been carried out to determine the chemical composition of the deposited film (Fig. 2 and Table 1).

Table 1. Composition of the applied electrodes, the wt.% of CuO in the prepared electrodes, the oxidation peak current density and peak potential for electrooxidation of 0.05 M glucose in 0.25 M NaOH at 50 mV s^{-1}.

Electrode	Content of CuO in the bath (g L^{-1})	Wt.% of CuO in the deposit from EDX	I_p, mA cm^{-2}	E_p, mV (MMO)
Massive Cu	-	-	28	858
Cu/C	-	-	44	818
Cu–CuO/C (I)	1	4	46	620
Cu–CuO/C (II)	3	10	55	637
Cu–CuO/C (III)	5	25	93	657
Cu–CuO/C (IV)	10	23	85	658

According to the obtained data, the wt.% CuO in Cu matrix increases with increasing CuO content in the electrolyte. It should be noticed that the wt.% of CuO reached a maximum value at 5 g L^{-1} CuO and then it slightly decreases with increasing the applied CuO content. This limiting concentration (5 g L^{-1}) may correspond to the steady state equilibrium, whereby the number of codepositing particles equals the number of particles approaching the carbon substrate. The decreasing trend of wt.% with further addition of CuO content in the electrolyte is attributed to the particles agglomeration in the electrolyte. This means that the entrapment of the CuO particles into the growing Cu matrix depends on the rate of CuO particles approaching to the cathode surface.

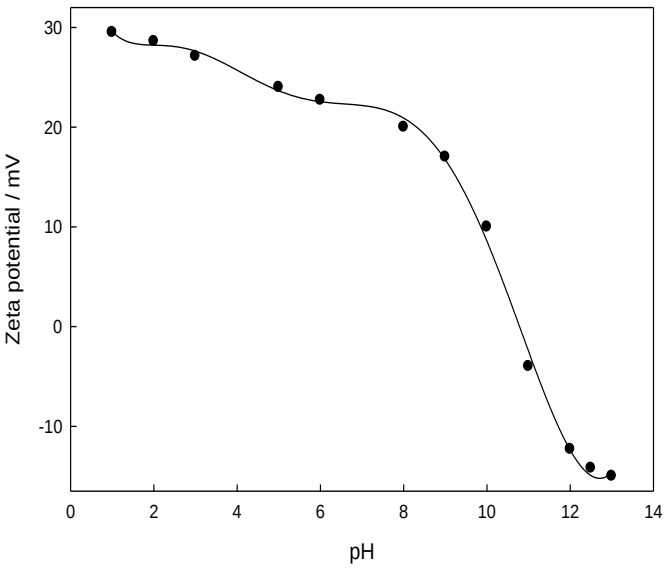

Figure 3. Variation of zeta potential of CuO particles with pH of the plating electrolyte.

The incorporated CuO can be attributed to the adsorption of suspended particles on the cathode surface, as suggested by Guglielmi's two-step adsorption mode [24]. Once the particle is adsorbed, the metal begins building around the cathode slowly, encapsulating and incorporating the particles. The co-deposition of particles and metal depends on Vander Waals force on the cathode surface according to the absorption theory [25, 26]. Moreover, the zeta potential of CuO particles at pH 12.5 has a negative value of ~ -14.2 mV as shown from Fig 3. The negative zeta potential of CuO is an effective factor in trapping the Cu^{2+} ions on to the surface of CuO powder in the plating electrolyte, so the amount of adsorbed Cu^{2+} increases as the amounts of CuO powder increases in the electrolyte. Further increasing of CuO powder beyond 5 g L^{-1} resulted in a slight decrease in the wt.% of CuO in the deposited film indicating that the adsorption of CuO particles in the film has reached the saturated level [27].

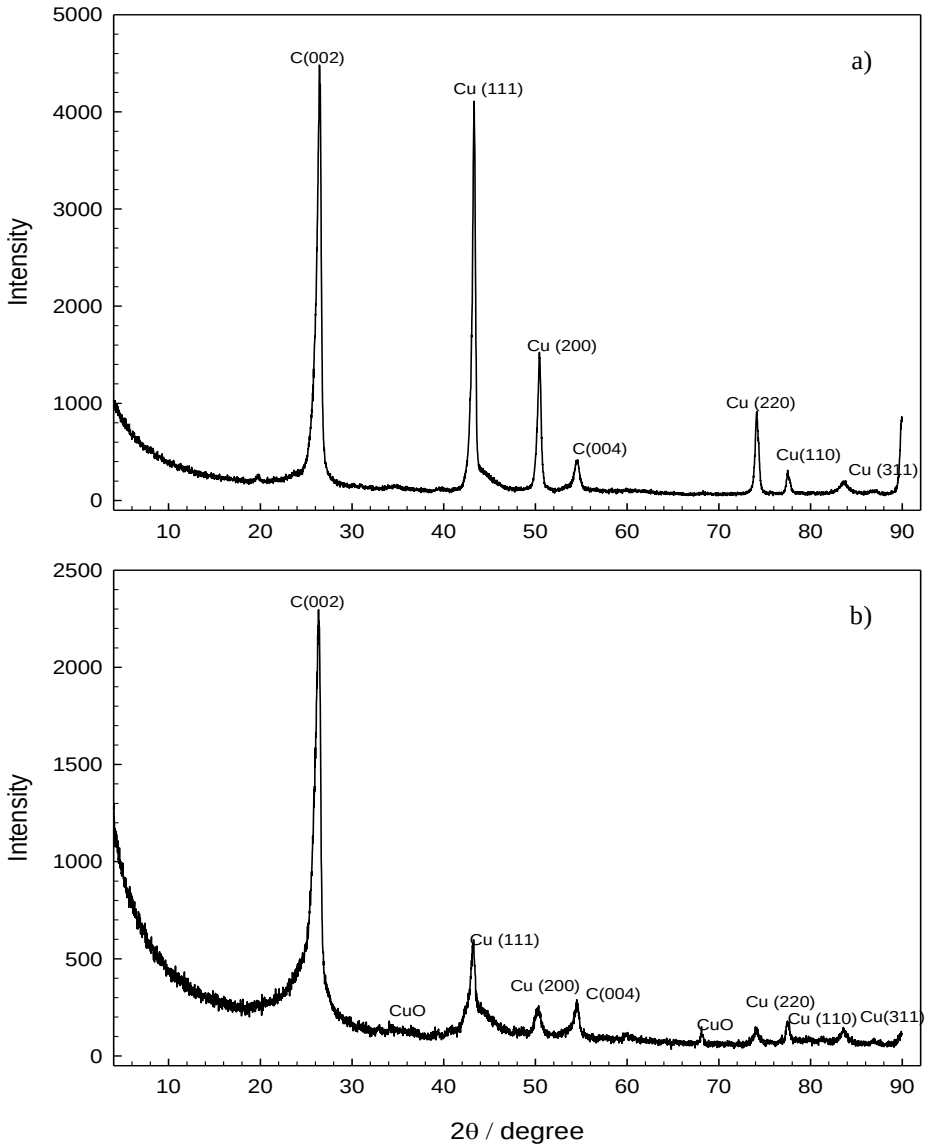

Figure 4. XRD patterns of a) Electrodeposited Cu/C and b) Cu–CuO/C film deposited at 5 g L^{-1} CuO in the electrolyte.

X-ray diffraction patterns of pure Cu matrix and Cu–CuO composite films are presented in Fig. 4. For pure Cu matrix (Fig. 4a), three main sharp peaks of high intensity for Cu are observed in the pattern with diffraction angles (2θ) at 43.3º, 50.4º and 74º corresponding to (111), (220) and (200) planes of the cubic Cu structure (JCPDS card no. 04-0836), respectively. The additional sharp peak of high intensity denoted in Fig. 4a at 2θ of 26.3º can be well indexed as the characteristic (002) plane of carbon. While, for Cu–CuO composite film (Fig. 4b), the same diffraction peaks of carbon and Cu are observed but with lower intensity, in addition two small peaks corresponding to CuO are detected at 2θ of 34º and 68º confirming the incorporation of CuO in the Cu matrix. It is worth noting that all pure Cu and Cu–CuO composite films are well-crystallized (Fig. 4). Nevertheless, the composites always presented a finer-grained Cu matrix. This means that the incorporation of CuO particles has an inhibiting effect on Cu grain growth. From calculations based on XRD (Fig. 4), it was found that the average size of Cu grain in the Cu–CuO composite films is about 11.2 nm while that of pure Cu is about 24.3 nm. Such decrease in grain size can be attributed to the distribution of CuO particulates on the boundaries of Cu grains, which restricts the growth of Cu grains in the deposition process and results in a fine grain surface [28]. Additionally, it is inferred that mannitol anions have a refining action similar to those obtained from glycerol–alkaline solutions [29].

3.2. Electrocatalytic activity and oxidation of glucose

The electrocatalytic activity of Cu–CuO/C electrodes was investigated in 0.25 M NaOH solutions and compared to those of the massive Cu and electrodeposited Cu/C electrodes. Typical cyclic voltammograms of massive Cu, electrodeposited Cu/C and Cu–CuO/C electrodes in 0.25 M NaOH solution in the potential range from –800 to +1200 mV (MMO) and at a potential sweep rate of 50 mV s^{-1} are shown in Fig. 5 (a– c). Both Cu/C and Cu–CuO/C were deposited at 4 A dm^{-2} and at 25 ^{o}C. From these cyclic voltammograms, it is clear that few numbers of well established peaks are observed in both anodic and cathodic half cycles. Three separate anodic oxidation peaks marked as Ia, IIa and IIIa were observed upon anodic sweeping of potential.

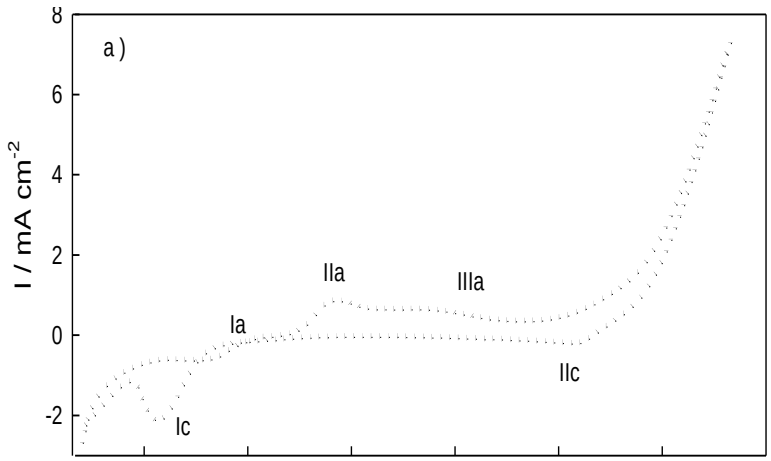

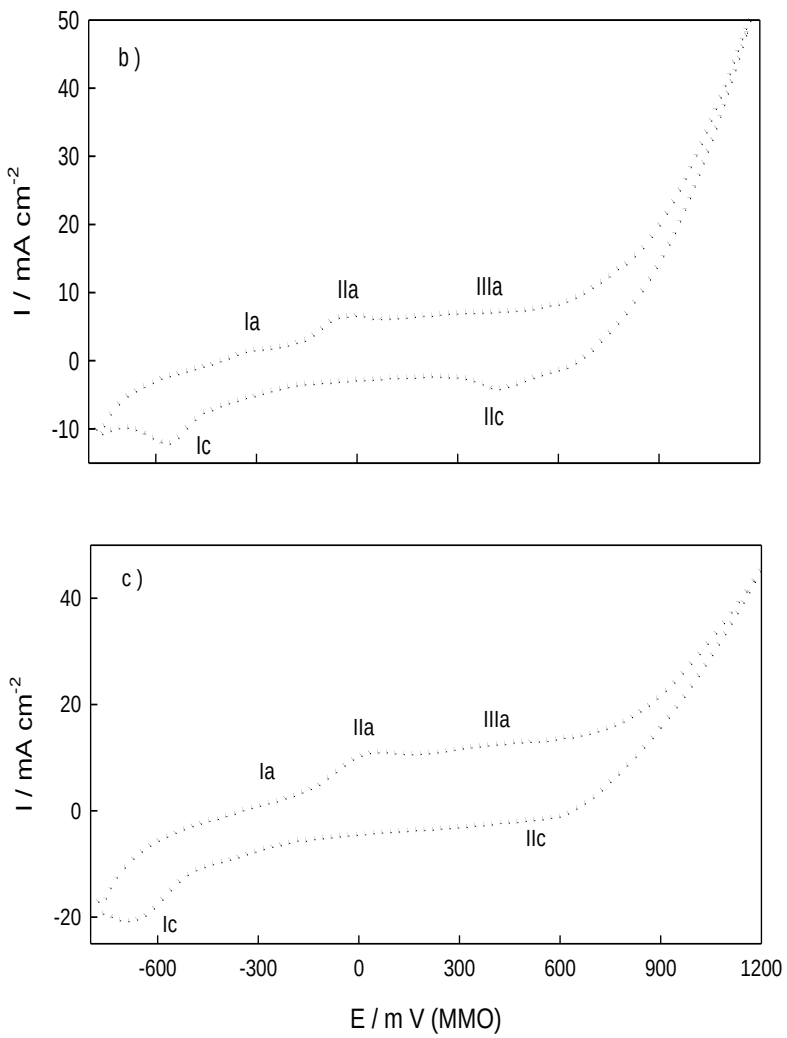

Figure 5. Cyclic voltammograms of: a) massive Cu and electrodeposited: b) Cu/C and c) Cu–CuO/C (25 wt.% CuO) in 0.25 M NaOH at a scan rate of 50 mV s^{-1}.

Comparing to the literatures [1, 30, 31], peak Ia in Fig. 5 is attributed to the Cu/Cu(I) redox species, it appears at potential values of about –260, –320 and –300 mV (MMO) for the massive Cu, Cu/C and Cu–CuO/C, respectively. At the working pH value of 12.5, Cu(I) hydroxide is the main product which is transformed to the corresponding oxide according to the following reactions [32]:

$$Cu + OH^- \rightarrow CuOH + e^- \qquad (1)$$

$$2CuOH \leftrightarrow Cu_2O + H_2O \qquad (2)$$

While, peak IIa in Fig. 5 is assigned to Cu/Cu(II) as well as Cu(I)/Cu(II) transitions through the following electrode processes [33]:

$$Cu + 2OH^- \rightarrow Cu(OH)_2 + 2e^- \qquad (3)$$

$$Cu_2O + H_2O + 2OH^- \rightarrow 2Cu(OH)_2 + 2e^- \quad (4)$$

$$CuO(OH)_2 \leftrightarrow CuO + H_2O \quad (5)$$

These redox species appear at potential values of about –20, –20 and +59 mV (MMO) for the massive Cu, Cu/C and Cu–CuO/C, respectively. In addition, peak IIIa is presumably corresponding to the Cu(II)/Cu(III) species which always appears in the course of the oxidation of copper as well as copper containing modified electrodes [22]. Also its peak potential is about +238, +279 and +418 mV (MMO) for the massive Cu, Cu/C and Cu–CuO/C, respectively. Moreover, peaks Ic and IIc in the cathodic half cycle are assigned to the reduction of Cu(I) to Cu and Cu(II) to Cu(I), respectively [31, 34]. From cyclic voltammograms Fig. 5(a– c), peak Ic that corresponds to the reduction of Cu(I) to Cu appears at potential values about –577, –578 and –697 mV (MMO) for the massive Cu, Cu/C and Cu–CuO/C, respectively and peak IIc which corresponds to the reduction of Cu(II) to Cu(I) species appears at potential values of about +599, +400 and +499 mV (MMO) for the massive Cu, Cu/C and Cu–CuO/C, respectively. Similar observation has been reported by Miller [35] in a ring-disk voltammetric study of Cu electrodes in alkaline solutions. Notably in our work, the cyclic voltammograms of the electrodeposited Cu/C or Cu–CuO/C in 0.25 M NaOH exhibited a higher current density of the redox species [Fig. 5(b, c)] compared with that of the massive Cu electrode as shown in Fig. 5a.

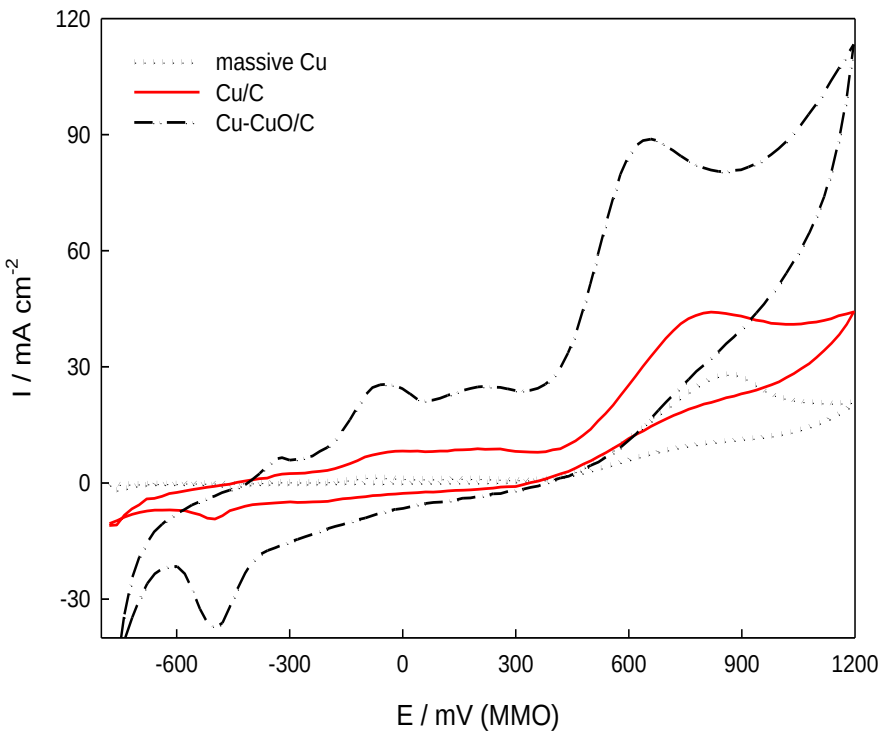

Figure 6. Cyclic voltammograms of electrooxidation of 0.05 M glucose at massive Cu, electrodeposited Cu/C and Cu–CuO/C (25 wt.% CuO) at 4 A dm^{-2} in 0.25 M NaOH at a scan rate of 50 mV s^{-1}.

After addition of 0.05 M glucose, an increase of anodic peak current corresponding to the irreversible glucose oxidation in the potential range from +500 to +800 mV (MMO) was observed as shown in Fig. 6. It represents the electrochemical oxidation of 0.05 M glucose at the massive Cu, electrodeposited Cu/C and Cu–CuO/C (25 wt.% CuO) electrodes in 0.25 M NaOH at a scan rate of 50 mV s^{-1}. The oxidation process starts at about +500 mV (MMO) reaching its maximum value at the peak in the anodic direction. Table 1 represents the oxidation peak current density and the peak potential values for electrooxidation of 0.05 M glucose in 0.25 M NaOH at the three electrodes. It is worth noting that the fabricated Cu–CuO/C composite electrode showed a higher oxidation current density and lower potential for glucose electrocatalytic oxidation in alkaline medium compared to the electrodeposited Cu/C or massive Cu electrodes. It seems that the presence of co-deposited CuO particles in Cu–CuO/C electrode is responsible for such enhancemnent.

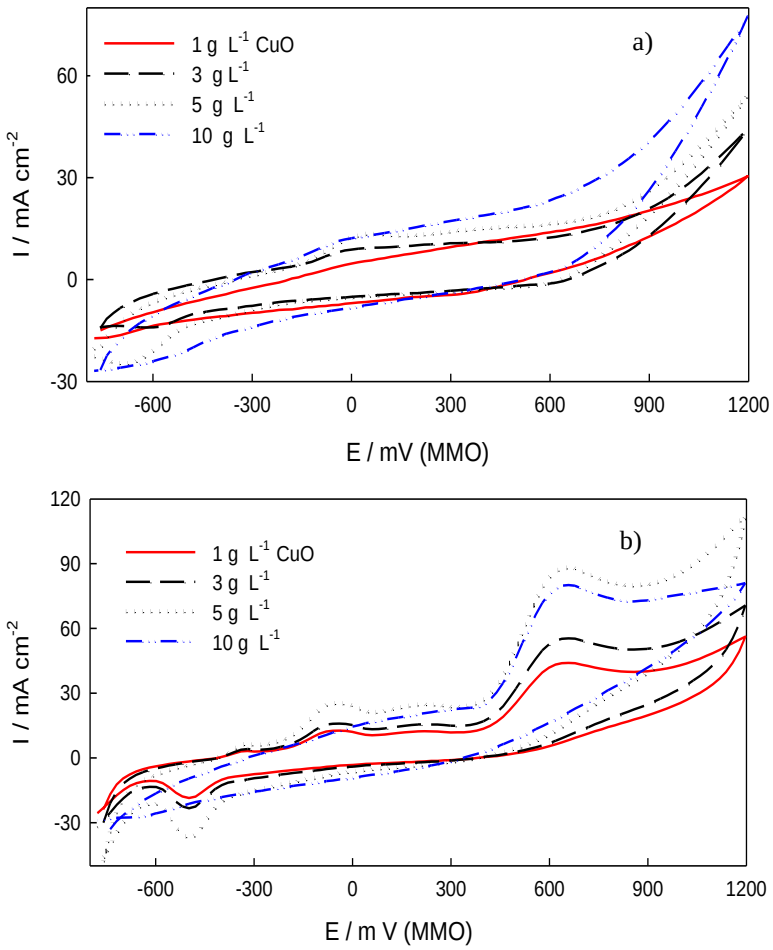

Figure 7. Cyclic voltammograms of electrodeposited Cu–CuO/C containing different amount of CuO in the deposition electrolyte at a scan rate of 50 mV s^{-1} in: a) 0.25 M NaOH and b) 0.25 M NaOH + 0.05 M glucose.

The role of CuO in enhancing the oxidation of glucose may discuss by finding that the presence of CuO reduces the size of Cu grain as calculated from XRD (Fig. 4) and thus increases the actual

surface area improving the catalytic activity towards electrooxdiation of glucose by increasing the number of active sites [36]. This finding is in agreement with Shi et al. assumption [37] which attributed the growth of the electrodeposited layer to a competition between the nucleation and crystal growth. Accordingly, CuO particles may provide more nucleation sites and hence retard the crystal growth; subsequently the corresponding Cu matrix in the composite film has a smaller crystal size.

Furthermore, the presence of CuO enhances the transformation of Cu^{2+}/Cu^{3+} species (this behavior is obvious from the cyclic voltammograms Fig. 5c). The Cu^{3+} ions are considered the main species necessary for glucose oxidation on Cu or Cu–based electrodes in alkaline solution as illustrated in equation 6. Also, the high performance of the proposed electrode may be attributed to its higher surface area compared with that of Cu/C electrode.

The effect of changing CuO content in the electrolyte (1– 10 g L^{-1}) on the electrocatalytic behavior of the fabricated electrodes in 0.25 M NaOH solution is illustrated in Fig. 7a. Notably, as the wt.% of CuO in the deposit film increases the height of the peak current densities of the redox species increases and the highest one was found for the Cu–CuO/C electrode that contains 25 wt.% CuO and prepared at electrolyte load of 5 g L^{-1} CuO (Fig. 7a.). The explanation of this behavior is owing to the negative zeta potential of CuO in the plating electrolyte which leads to increase the amount of adsorbed Cu^{2+} ions on the surface of CuO particles and result in deposition of a large amount of Cu. Additionally, the presence of CuO particles reduces the Cu grain size thus increasing the actual surface area of the electrode. Moreover, it enhances the transformation of Cu^{2+}/Cu^{3+} redox species.

The same observation was obtained in presence of 0.05 M glucose (Fig. 7b), it is worth noting that as the amount of CuO in the prepared electrode increases the oxidation peak current density of glucose increases (as the amount of Cu^{2+}/Cu^{3+} redox species increases as mentioned before) and reaching a maximum value at 5 g L^{-1} CuO. Further increase in CuO content up to 10 g L^{-1} in the electrolyte results in a slight decrease in the wt.% of CuO in the prepared electrode and hence the oxidation peak current density of glucose slightly decreases, as the Cu particles may aggregate at high content of CuO. The best result regarding the oxidation peak current density of glucose is obtained with Cu–CuO/C (25 wt.% CuO) [93 mA cm^{-2} at 657 mV(MMO)] compared to the other fabricated electrodes as shown in Table 1.

Ortiz et al. [38] assumed that the electrooxidation of organic compounds (e.g. glucose) in alkaline medium requires the presence of oxide, hydroxide and /or oxyhydroxide groups. According to this assumption, the oxidation process of glucose at Cu or Cu composite electrodes starts at a potential value corresponding to the formation of CuOOH species and the oxidation process starts as Cu(III) species is formed. It was suggested that, glucose is oxidized on the Cu or Cu composite electrodes through the reaction with CuOOH to form $Cu(OH)_2$:

$$CuOOH + \text{glucose} \leftrightarrow Cu(OH)_2 + \text{oxidation products} \qquad (6)$$

On the other hand, Fleishmann et al. [39] reported that the oxidation reaction of organic compounds with oxides of higher valences is usually the rate-determining step. So, the above equation 6 is the slow step for glucose oxidation process in alkaline solutions at Cu or Cu composite electrodes.

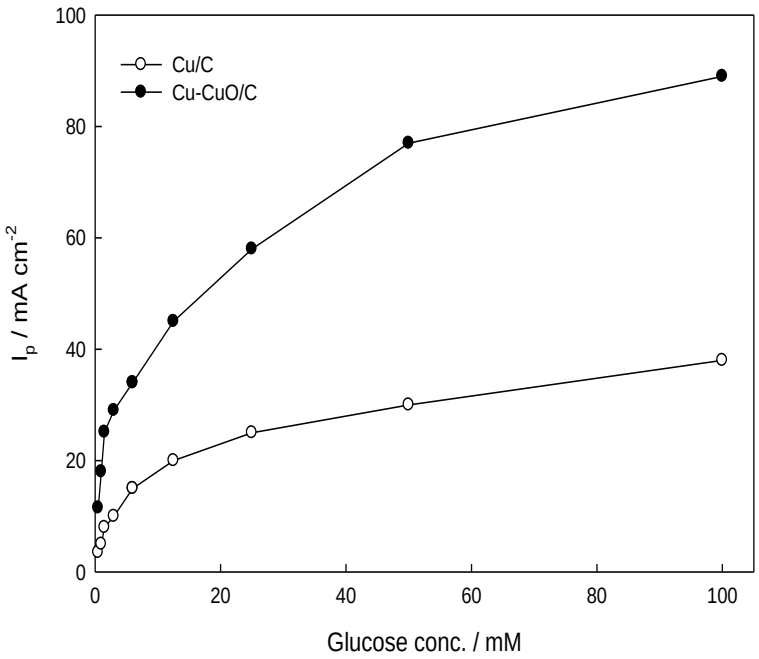

Figure 8. Relation between the oxidation peak current density of glucose at various glucose concentrations in 0.25 M NaOH at 50 mV s^{-1} in 0.25 M NaOH at: ○) Cu/C and ●) Cu-CuO/C (25 wt.% CuO).

Figure 8 shows the relationship between the oxidation peak current density of glucose and glucose concentrations in the range from 0.5 mM to 100 mM in 0.25 M NaOH at Cu/C and Cu–CuO/C electrodes. The oxidation peak current density of glucose increases with increasing glucose concentration at the two studied electrodes. But, it is worth noting that Cu–CuO/C composite electrode displayed a higher oxidation peak current density for glucose oxidation at various glucose concentrations compared with Cu/C electrode. The crucial factor for the glucose oxidation at the Cu–based electrode in the alkaline solution is the formation of CuOOH species, and any conditions favoring this process lead to enhancing glucose oxidation, so the presence of CuO in Cu–CuO/C electrode enhances the formation of CuOOH and accordingly the oxidation peak current density of glucose increases.

3.3. Chronoamperometry and detection of glucose

The amperometric response of Cu–CuO/C electrode was observed at +750 mV with successive additions of glucose and the solution is stirred constantly and it is compared with that of electrodeposited Cu/C electrode. The calibration curve for glucose sensor is shown in Fig. 9 at Cu/C and Cu–CuO/C (25 wt.% CuO), respectively. Two linear regions of glucose concentrations for the two studied electrodes were noticed. In the first linear region, the response increases rapidly with the concentration of glucose. However, the adsorption of intermediates could occur after a certain time resulting in the slow down of the current increase. The sensitivity of Cu–CuO/C (25 wt.% CuO)

electrode was evaluated showing a linear range up to 3 mM glucose with sensitivity of 598 μA cm^{-2} mM^{-1} and detection limit of 5 μM. The sensitivity value of this electrode is about twice that of the electrodeposited Cu/C electrode (319 μA cm^{-2} mM^{-1}) prepared at the same conditions.

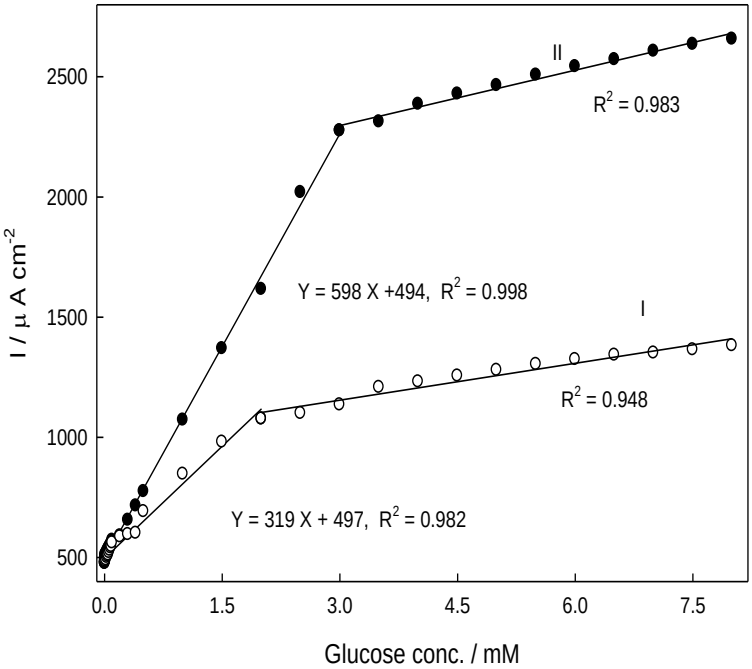

Figure 9. Calibration curves for amperometric detection of glucose at +750 mV in 0.25 M NaOH at different glucose concentrations at electrodeposited: I) Cu/C and II) Cu-CuO/C (25 wt.% CuO).

Moreover, Cu–CuO/C electrodes showed an improved performance towards the electrooxidation process with time compared to the massive Cu or Cu/C electrodes. To indicate the stability of the various prepared electrodes towards electrooxidation of glucose, the chronoamperometric experiments for the massive Cu, Cu/C and Cu–CuO/C elctrodes were performed at +750 mV (MMO) and represented in Fig. 10a at 0.05 M glucose in 0.25 M NaOH. In comparison with the massive Cu or Cu/C, the Cu–CuO/C electrode delivers a high steady state oxidation current density and better stability due to the promoting effect of the CuO. CuO may prevent the poisoning of the electrode by the intermediate species of glucose oxidation. Moreover, Plotting of the net current with respect to the inverse of the square roots of time represents a straight line as shown in Fig. 10b. The dominance of a diffusion controlled process is evident, using the slope of this line in Cottrell equation [40]:

$$I = nFAD^{1/2} C\pi^{-1/2} t^{-1/2} \qquad (7)$$

Where, n is the number of transferred electrons, F is the Faraday constant which equals ~ 96500 C $mol.^{-1}$, A is the surface area, D is the diffusion coefficient of glucose and C is the

concentration. The slope of these lines (Fig. 10b) revealed that the surface area of Cu–CuO/C (25 wt.% CuO) electrode is about twice that of electrodeposited Cu/C electrode, so the presence of CuO particles increases the actual surface area of the prepared electrode and accordingly increases its electrocatalytic activity.

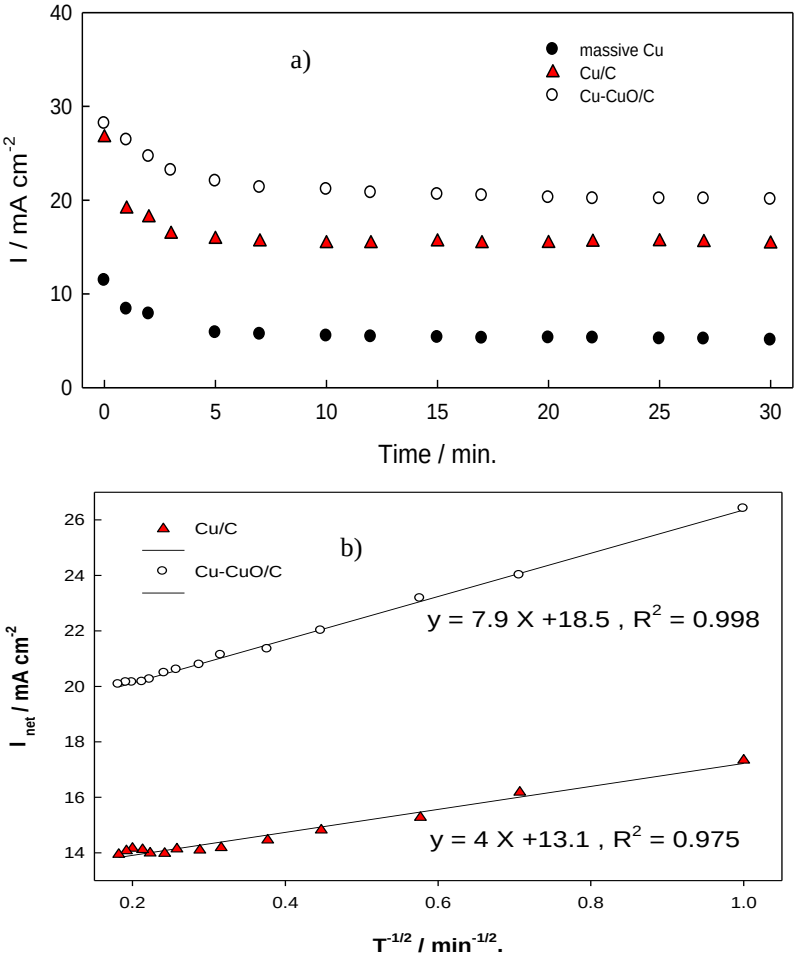

Figure 10. a) Chronoamperometry of different electrodes at +750 mV (MMO) in 0.25 M NaOH + 0.05 M glucose and b) Relation between the net current and the inverse of the square roots of time.

3.4. Effect of interfering species

Cu–CuO/C electrode is thought to be selective to glucose in the presence of some common interfering species that present in biological fluids such as ascorbic acid. The normal physiological level of glucose is about 3– 8 mM, which is much higher than the concentration of any interfering species such as ascorbic acid (0.1 mM) [41, 42]. Electrocatalytic activity of Cu–CuO/C towards oxidation of ascorbic acid in 0.25 M NaOH solution was examined using the cyclic voltammetric technique in the same potential window of glucose oxidation from –800 to +1200 mV (MMO) at a scan rate of 50 mV s^{-1} and represented in Fig. 11. No appreciable oxidation peak was observed for ascorbic acid up to 2.0 mM, this concentration value exceeds the normal level of ascorbic acid in

human blood. On the other hand, the performance of this electrode towards electrooxidation of glucose at lower concentration down to 0.5 mM imparts an appreciable oxidation peak for glucose as shown in Fig. 11. This indicates the selectivity of the fabricated Cu–CuO/C towards glucose oxidation.

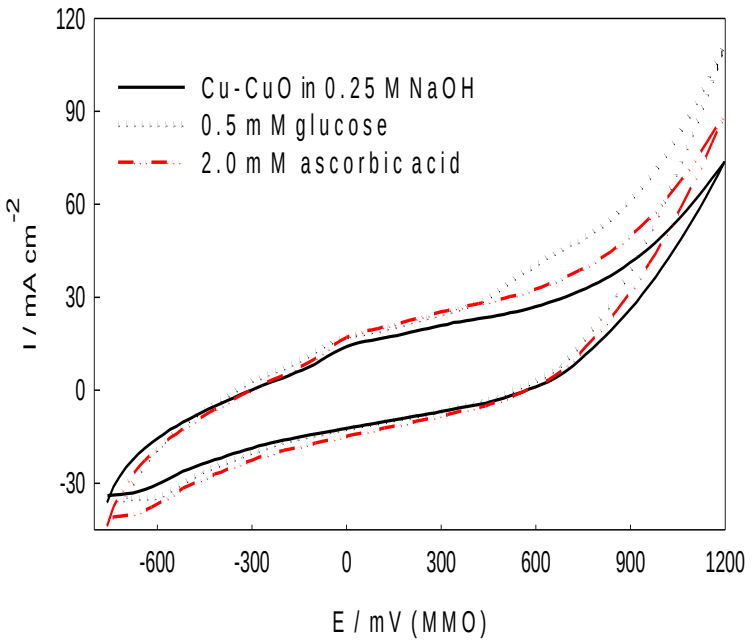

Figure 11. Cyclic voltammograms of electrodeposited Cu–CuO/C (25 wt.% CuO) at a scan rate of 50 mV s^{-1} in 0.25 M NaOH in presence of 0.5 mM glucose and in presence of 2.0 mM ascorbic acid.

Eventually, in comparison with the electrodeposited Cu/C, the Cu–CuO/C composite electrode exhibited a higher catalytic activity and better stability towards electrooxidation of glucose in 0.25 M NaOH solution. Moreover, the sensitivity value of the Cu–CuO/C composite electrode (~598 μA cm^{-2} mM^{-1}) is about twice as that of the electrodeposited Cu/C electrode (~319 μA cm^{-2} mM^{-1}) prepared at the same conditions. In addition, its sensitivity is comparable to or even better than those of some reported glucose sensors such as CuO nanospheres electrode of a sensitivity ~ 404.5 μA cm^{-2} mM^{-1} [43], CuO nanorod electrode of a sensitivity ~ 450 μA cm^{-2} mM^{-1}, CuO nanowires of a sensitivity ~ 490 μA cm^{-2} mM^{-1}, CuO/Nafion/GC of a sensitivity ~ 400 μA cm^{-2} mM^{-1} [44] and self assembled CNT thin films with Cu nanoparticles electrode of a sensitivity ~ 602 μA cm^{-2} mM^{-1} [45]. Moreover, owing to the low cost and ease of fabrication method, Cu–CuO/C composite electrode is thought to be active electrocatalyst for glucose sensor manufacturing.

4. CONCLUSIONS

Cu–CuO composite films have been successfully fabricated on carbon electrodes via an electrodeposition route from an environmentally safe alkaline electrolyte containing manntiol as a

complexing agent. XRD patterns showed that the presence of CuO reduces the Cu grain from 24.3 to 11.2 nm. The electrochemical studies reveled that the performance of Cu–CuO/C composite electrode towards glucose electrooxidation is superior to that of electrodeposited Cu/C electrode in alkaline solution. Also, its stability with time is better than that of Cu/C electrode. The proposed composite electrode has reasonable sensitivity and selectivity towards glucose electrooxidation. Owing to its safe and simple fabrication technique, it is recommended to be used for the development of enzyme-free glucose sensors.

References

1. H. Heli, M. Jafarian, M. G. Mahjani, F. Gobal, *Electrochim. Acta*, 49 (2004) 4999.
2. N. Torto, T. Ruzgas, L. Gorton, *J. Electroanal. Chem.*, 464 (1999) 252.
3. H. Wu, W-M. Cao, Y. Li, G. Liu, Y. Wen, H-F. Yang, Yang S-P., *Electrochim. Acta*, 55 (2010) 3734.
4. J. Zhao, F. Wang, J. Yu, S.Hu, *Talanta*, 70 (2006) 449.
5. T-K. Huang, K-W. Lin, S-P. Tung, T-M. Cheng, C. Chang, Y-Z. Hsieh, C-Y. Lee, H-T.Chiu, *J. Electroanal. Chem.*, 636 (2009) 123.
6. K. M. El-Khatib, R. M. Abdel Hameed, *Biosens. Bioelectron.*, 26 (2011) 3542.
7. L. A. Colon, R. Dadoo, R. N. Zare, *Anal. Chem.*, 65 (1993) 476.
8. H. Pang, Q. Lu, J. Wang, Y. Li, F. Gao, *Chem. Commun.*, 46 (2010) 2010.
9. I-H. Yeo, D. C. Johnson, *J. Electroanal. Chem.*, 495 (2001) 110.
10. F. Matsumoto, M. Harada, N. Koura, S. Uesugi, *Electrochem. Commun.*, 5 (2003) 42.
11. J. Wang, P. V. A. Pamidi, G. Cepria, *Anal. Chim. Acta*, 330 (1996) 151.
12. C. B. McAuley, C. G. Wildgoose, R. G. Compton, C. L. Shao, M. L. H. Green, *Sens. Actuators B*, 132 (2008) 356.
13. L. Hu, L. S. Chi, N. K. Goh, S. N. Tan, *Electroanalysis*, 12 (2000) 2871.
14. C. Li, Y. Zhang, X. Lv, H. Xi, Y. Wang, *Biosens. Bioelectron.*, 26 (2010) 903.
15. T. G. Satheesh Babu, T. Ramachandran, *Electrochim. Acta*, 55 (2010) 1612.
16. X. Wang, C. Hu, H. Liu, G. Du, X. He, Y. Xi, *Sens. Actuators B*, 144 (2010) 220.
17. H. Matsubara, T. Kondo, W. Kanno, K. Hodouchi, A. Yamada, *Anal. Chim. Acta*, 405 (2000) 87.
18. T. You, O. Niwa, M. Tomita, H. Ando, M. Suzuki, S. Hirono, *Electrochem. Commun.*, 4 (2002) 468.
19. K. S. Ashok, H-W. Cheng, S-M. Chen, S-F. Wang, *Mat. Sci. Eng.* C, 30 (2010) 86.
20. S. T. Farrell, C. B. Breslin, *Electrochim. Acta*, 49 (2004) 4497.
21. F. A. Lowenheim, Modern Electroplating, Wiley USA, New York (1974).
22. I.G. Casella, M. Gatta, *J. Electroanal. Chem.*, 494 (2000) 12.
23. Z. Abdel Hamid, A. Abdel Aal, *Surf. Coat. Tech.*, 203 (2009) 1360.
24. N. Guglielmi, *J. Electrochem. Soc.*, 119 (1972) 1009.
25. R. Xu, J. Wang, L. He, Z. Guo, *Surf. Coat. Tech.*, 202 (2008) 1574.
26. J. Fransaer, J. P. Celis, J. R. Roos, *J. Electrochem. Soc.*, 1992 (139) 413.
27. A.Abdel Aal, M. Bahgat, M. Radwan, *Surf. Coat. Tech.*, 201 (2006) 2910.
28. H. B. Hassan, Z. Abdel Hamid, *Int. J. Hydrogen Energy*, 36 (2011) 849.
29. M. R. H. Almeida, I. A. Carlos, L. L. Barbosa, R. M. Carlos, B. S. Lima-Neto and E. M. J. A. Pallone., *J. Appl. Electrochem.*, 32 (2002)763.
30. M. Z. Luo, R. P. Baldwin, *J. Electroanal. Chem.*, 387 (1995) 87.
31. J. M. Marioli, T. Kuwana, *Electrochim. Acta*, 37 (1992) 1187.
32. C. H. Pyun, S. M. Park, *J. Electrochem. Soc.*, 132 (1986) 2024.
33. S. M. Abd El-Haleem, B. G. Ateya, *J. Electroanal. Chem.*, 117 (1981) 309.

34. L. D. Burke, M. J. G. Ahern, T. G. Ryan, *J. Electrochem. Soc.*, 137 (1990) 553.
35. B. Miller, *J. Electrochem. Soc.*, 116 (1969) 1675.
36. S. M. A. Shibli, V. S. Dilimon, *Int. J. Hydrogen Energy*, 32 (2007) 1694.
37. L. Shi, C. Sun, P. Gao, F. Zhou, W. Liu, *Appl. Surf. Sci.*, 252 (2006) 3591.
38. R. Ortiz, O. P. Marquez, J. C. Gutierrez, *J. Phys. Chem.*, 100 (1996) 8389.
39. M. Fleischmann, K. Korinek, D. Pletcher, *J. Chem. Soc. Perkin* II, 2(10) (1972) 1396.
40. A.J. Bard, L. R. Faulkner, editor. Electrochemical methods, fundamentals and applications, Wiley; New York (2001) p. 209 chapter 5.
41. X. Kang, Z. Mai, X. Zou, P. Cai, J. Mo, *J. Anal. Biochem.*, 363 (2007) 143.
42. A.Safavi, N. Maleki, E. Farjami, *Biosens. Bioelectron.*, 24 (2009) 1655.
43. E. Reitz, W. Jia, M. Gentile, Y. Wang, Y. Lei, *Electroanalysis*, 20 (2008) 2482.
44. K. E. Toghill, L. Xiao, M. A. Phillips, R. G. Compton, *Sens. Actuators B*, 147 (2010) 642.
45. X. Li, Q. Zhu, S. Tong, W. Wang, W. Song, *Sens. Actuators B*, 136 (2009) 444.

© 2011 by ESG (www.electrochemsci.org)